D. Kogut et al.

Hydrogen Isotope Exchange in Beryllium: Modelling and Experiment

(18th May 2015 – 22nd May 2015)
Aix-en-Provence, France

Hydrogen isotope exchange in beryllium: modelling and experiment

D Kogut[1,*], D Douai[2], M J Baldwin[3], R P Doerner[3], D Sinelnikov[4], N Mamedov[4], V Kurnaev[4], H W Becker[5] and T Schwarz-Selinger[6]

[1]Aix-Marseille Université, CNRS, PIIM, UMR 7345, 13013 Marseille, France

[2]CEA Cadarache, IRFM, 13108 St. Paul lez Durance, France

[3]UCSD, Center for Energy Research, 9500 Gilman Drive, La Jolla, CA 92093-0417, USA

[4]National Research Nuclear University «MEPhI», 115409 Moscow, Russia

[5]Ruhr-Universität Bochum, RUBION, D-44801 Bochum, Germany

[6]Max-Planck-Institut für Plasmaphysik, Boltzmannstr. 2, D-85748 Garching, Germany

Abstract

In order to understand the interaction mechanisms between hydrogenic species and beryllium co-deposits, a 1D Diffusion Trapping Model of Isotopic eXchange in Be (DITMIX) is developed. Hydrogen profiles from DITMIX are in a good agreement with profiles measured by ^{15}N-NRA on pre-characterized 600 nm thick Be:H layers, which were irradiated by D ions with well-defined fluxes and energies, for different fluences and surface temperatures. Hence DITMIX provides a qualitative understanding of the isotope exchange mechanisms, although modelled vs. measured D profiles show less agreement in the bulk, casting some doubt on the processes involved. DITMIX shows that the main factors determining isotopic exchange are the irradiation fluence and the surface temperature.

PACS: 52.40.Hf; 52.77.Dq; 67.63.-r; 73.50.-h; 81.15.Jj

---

* Corresponding author; e-mail: dmitry.kogut@univ-amu.fr

1. Introduction

Wall conditioning by low temperature plasmas in ITER, such as glow discharges (GDC) during maintenance phases or discharges created by the ion cyclotron radio frequency (ICWC) between plasma pulses in the presence of the magnetic field, will contribute to the tritium inventory control. The major cause of tritium retention in ITER is erosion and co-deposition of the plasma-facing materials with fuel [1]. Experimental evidence from JET with ITER-like Wall suggests that the fuel implantation in Be and W dominates at first followed by fuel co-deposition with Be on top of the divertor tiles [2-4]; hence it is important to assess how deep such co-deposits can be accessed by conditioning techniques.

It was shown that isotopic exchange is a promising technique to eliminate tritium from the walls by replacing it with deuterium from the conditioning plasma [5]. H_2-ICWC on the JET-ILW preloaded by D_2 tokamak operation is estimated to remove $7.3 \cdot 10^{22}$ D atoms within 400 s of cumulated operation time [6], which is quite efficient given the maximum deuterium retention rate of $1.5 \cdot 10^{20}$ D/s in JET-ILW [2]. The extrapolated values of tritium removal by the inter-pulse ICWC in ITER are comparable with expected retention in a nominal DT plasma pulse [5].

However, the mechanisms involved in hydrogen isotope exchange are still poorly understood at a microscopic level, in terms of particle interaction with beryllium and there is no specific theory or model in the literature. A 1D Diffusion Trapping Model for Isotopic eXchange (DITMIX) has been developed, based on existing approaches to simulate the hydrogen transport in metals [7-9]. The model is validated through comparison with the experimental data obtained under well-controlled conditions. This paper presents insight into the processes involved in hydrogen isotope change-over provided by DITMIX. Conclusion is offered with regard to the efficiency of isotope exchange in ITER.

2. The DITMIX model

DITMIX is based on transport equations of hydrogen in metals such as used in TMAP and in other codes [7-9]. It solves a system of partial differential equations and computes a 1D time-dependent solution for concentrations of dissolved and trapped hydrogen isotopes in beryllium. The diffusion-trapping parameters and the surface recombination model are taken from recent simulations of thermal D release from Be co-deposits which proved to be in excellent agreement with experimental TDS spectra [10].

The co-deposited Be:H:D film is simulated by a 1D layer of thickness L, divided into N_x computational nodes. The nodes are non-uniformly distributed over the layer with the grid refinement in the subsurface layers in order to resolve strong concentration gradients which develop there. The tungsten substrate is not simulated as hydrogen retention and transport are very limited in W

compared to Be co-deposit [11]. Impurities at the surface such as thin oxide layer of BeO are also neglected, although the latter may act as an additional transport barrier for hydrogen and reduce surface recombination rate [12]. The model considers two species of hydrogen – H and D, which are denoted here by indexes i or j. Each isotope is represented by two types of populations: soluted (mobile) particles with concentration $u_i(x,t)$ and trapped (immobile) particles with concentration $w_i^k(x,t)$, where index k denotes the type of trapping site. Only one isotope is allowed in each trapping site, although some DFT calculations predict multiple hydrogen trapping (up to 5 atoms) in a single vacancy [14].

The hydrogen transport in the film is controlled by the following diffusion equation:

$$\frac{\partial u_i(x,t)}{\partial t} = \frac{\partial}{\partial x}\left(D(x,t)\frac{\partial u_i}{\partial x}\right) + \Phi_i(x,t) - \sum_k \frac{\partial w_i^k(x,t)}{\partial t}.$$

(1)

The first term on the right-hand-side is a diffusion term, where $D(x,t) = D_0 \exp(-E_d/kT(x,t))$ with pre-factor D_0 and activation barrier E_d; $T(x,t)$ is the local temperature and k is the Boltzmann constant. The second term stands for implantation profile:

$$\Phi_i(x,t) = \frac{1}{2}\operatorname{erfc}\left(\frac{t-t_{imp}}{\tau}\right) \cdot J_{0i}(1-R_i)\frac{dN_i(x)}{dx},$$

(2)

where J_{0i} is the incident flux of particles of type i, R_i – the particle reflection coefficient, the implantation profile $\frac{dN_i(x)}{dx}$ normalized per one incident projectile is taken from SCATTER [13] calculations, erfc is the complementary error function with parameter $\tau = \min(1, 0.1 t_{imp})$, introduced for numerical reasons. It is assumed that implantation is switched on at the moment $t = 0$ and off at $t = t_{imp}$.

The third term on the right-hand-side in equation (1) is the trapping rate term summarized over all available traps. It is defined by

$$\frac{\partial w_i^k(x,t)}{\partial t} = v_t^k \frac{u_i}{n_{Be}}\left[w_{max}^k - \sum_j w_j^k\right]\exp\left(-\frac{E_t^k}{kT(x,t)}\right) - v_r^k w_i^k \exp\left(-\frac{E_r^k}{kT(x,t)}\right) - w_i^k \Omega_{kin} - \Omega_{swap}^{i,k}.$$

(3)

Here n_{Be} is the volume density of Be, v_t^k is the trapping frequency; the trapping barrier E_t^k is assumed to be equal to the diffusion barrier E_d. w_{max}^k is the concentration of trapping sites of type k, including both filled and empty ones. The second term in equation (1) is thermal release (de-trapping) with characteristic attempt frequency v_r^k and detrapping barrier E_r^k.

The third term Ω_{kin} on the right-hand-side in equation (3) is introduced to simulate kinetic detrapping and subsequent isotopic exchange in the implantation zone. It is given by

$$\Omega_{kin}(x,t) = \sigma_{kin}\frac{1}{2}\text{erfc}\left(\frac{t-t_{imp}}{\tau}\right)\cdot\sum_j J_{0j}(1-R_j)\left[1-\int_0^x\frac{\mathrm{d}N_j(x)}{\mathrm{d}x}\mathrm{d}x\right],$$ (4)

here σ_{kin} is the cross-section of the hydrogen isotope release by an impact of energetic particle; it is assumed to be independent of the species type and of the order of square of Be inter-atomic distance, i.e. 10^{-16} cm^2. The cross-section is multiplied by the total flux term of the implanted species, which passes through the given point inside the material.

The fourth term $\Omega_{swap}^{i,k}$ on the right-hand-side in equation (3) is the "swapping" term introduced to simulate enhanced isotopic exchange all over the depth of the Be:H:D coating. This thermally activated process allows accounting for the probability that a soluted isotope is exchanged with a trapped one. This is a simplified approach to simulate a two-step exchange by multiple hydrogen trapping in a monovacancy: as a soluted isotope gets into a trap raising its fill level, the de-trapping barrier consequently decreases and another isotope has a chance to escape [14,15]. In case of two isotope species i = H and D, the swapping term is the following:

$$\Omega_{swap}^{H,k} = -\Omega_{swap}^{D,k} = \nu_t^k\exp\left(-\frac{E_{swap}^k}{kT(x,t)}\right)\left[u_\text{H}w_\text{D}^k - u_\text{D}w_\text{H}^k\right],$$ (5)

E_{swap}^k is the activation barrier for the swapping process.

On the rear side of the layer ($x = L$) the boundary condition of zero hydrogen flux is imposed, which may be justified by the fact of poor H solubility in W and negligible amount of intrinsic traps in tungsten substrate compared to Be co-deposit [11]. The boundary conditions on the front side ($x = 0$) are given by the balance of fluxes:

$$J_{ads}^i - J_{rec}^i = -\lambda\left(\frac{\partial u_i(0,t)}{\partial t} - \sum_k\frac{\partial w_i^k(0,t)}{\partial t}\right) + D(0,t)\frac{\partial u_i(0,t)}{\partial x} + \lambda\Phi_i(0,t).$$ (6)

λ is the Be lattice constant (2.29 Å). The surface flux of the hydrogen species i on the left hand side is defined by the difference of adsorption flux J_{ads}^i and recombination flux J_{rec}^i. It is assumed that J_{ads}^i is equal to the flux of incident molecules, i.e. the sticking coefficient is unity. Indeed, in the experiment the adsorption flux is negligible with respect to recombination and implantation fluxes. The molecular flux to the surface from the gas phase is given by the Hertz-Knudsen equation:

$$J_{ads}^i = \sum_j\frac{(1+\delta_{ij})p_{ij}}{\sqrt{2\pi M_{ij}kT_{gas}}}.$$ (7)

Here δ_{ij} is the Kronecker delta, p_{ij} is the partial pressure of the molecule ij in the vessel (H$_2$, HD or D$_2$), M_{ij} – the mass of the molecule ij, T_{gas} – the average gas temperature in the vessel.

The particle recombination flux J_{rec}^i is defined by the sum of molecular recombination fluxes:

$$J_{rec}^i = \sum_j(1+\delta_{ij})K_{rec}^{ij}u_i(0,t)u_j(0,t).$$ (8)

The recombination coefficient K_{rec}^{ij} is chosen according to the dynamically computed surface concentration (DSC) form, proposed in [10] to simulate the thermal desorption spectra from similar Be:D co-deposits.

The thermal response of the co-deposit layer is calculated via the heat conduction equation:

$$\rho_{Be} C_p \frac{\partial T(x,t)}{\partial t} = \frac{\partial}{\partial x}\left(\kappa \frac{\partial T(x,t)}{\partial x}\right) \tag{9}$$

Here ρ_{Be} is the mass density of the material, C_p is the specific heat and κ is the thermal conductivity. The boundary conditions are the following: $\partial T(L,t)/\partial x = 0$ and $T(0,t)$ is either fixed or evolves with time following a given scenario.

At the beginning of the simulations the soluted hydrogen concentration is $u_i(x,0) = 0$, while the trapping concentrations are given by initial trap occupancies f_i^k, so that $w_i^k(x,0) = f_i^k w_{max}^k$. The initial profile $w_i^k(x,0)$ is derived from experimental depth profiles.

Trap, $k = 1$ (intrinsic)	Trap, $k = 2$ (intrinsic)	Trap, $k = 3$ (ion-induced)
$w_{max}^1 = 0.027 n_{Be}$	$w_{max}^2 = 0.011 n_{Be}$	$w_{max}^3 =$ Fluence (10^{21}at/m^2)$\cdot 0.068 n_{Be}$
$f_H^1 = 0.944$	$f_H^2 = 1.0$	$f_H^3 = 0$
$f_D^1 = 0$	$f_D^2 = 0$	$f_D^3 = 0$
$E_t^1 = E_d = 0.364$ eV	$E_t^2 = E_d = 0.364$ eV	$E_t^3 = E_d = 0.364$ eV
$E_r^1 = 0.790$ eV	$E_r^2 = 0.978$ eV	$E_r^3 = 2.0$ eV
$\nu_t^1 = \nu_r^1 = 4\cdot 10^{12}$ s^{-1}	$\nu_t^2 = \nu_r^2 = 4\cdot 10^{12}$ s^{-1}	$\nu_t^3 = \nu_r^3 = 4\cdot 10^{12}$ s^{-1}

Table 1. Hydrogen trapping parameters in the DITMIX model

The parameters used in simulations for the thermal properties of Be and hydrogen transport in the Be layer are taken from [10]. The trapping parameters have been adjusted to simulate the experimental profiles which are discussed in the following sections (see Table 1).

The DITMIX model was benchmarked against the thermal desorption spectra published in [10]; it can perfectly reproduce the experimental data on the deuterium thermal release flux from Be:D co-deposits as a function of temperature.

3. Experimental procedure

Beryllium was deposited on W substrates (10mm×5mm×1mm) with root mean squared roughness of 100 nm, annealed at 1273 K beforehand, with hydrogen in the magnetron chamber at UCSD (as described in [10]). A gas mixture of Ar + H$_2$ at 0.8 Pa was used; the argon ions sputtering beryllium target and providing a deposition source of Be atoms. Resulting co-deposits contain trapped hydrogen

at the levels of H/Be ≈ 0.04–0.15, depending on the deposition conditions: an incident sputtered Be flux (~10^{19} m^{-2}s^{-1}), bias applied to the sample (-100 V), its surface temperature (100 °C), gas flow and Ar/H$_2$ ratio. Samples with 600 nm thick Be:H coatings with H/Be = 0.04 were produced for the H → D exchange experiments. The roughness of the tungsten substrates was necessary for a good adhesion and to prevent flaking of the deposed Be:H coating.

Isotopic exchange experiment was performed in the ion beam facility "Big Mass-Monochromator" (BMM) in MEPhI, Moscow [16]. Deuterium ions are produced in a duoplasmatron hot filament discharge source, accelerated with a well-defined energy and separated with the magnet by mass-to-charge ratio. The typical ion energies range between 1 and 40 keV, the ion flux on the target is ~1 µA/cm^2, i.e. ~10^{17} m^{-2}s^{-1}. Base pressure in the experimental chamber is below 10^{-6} Pa.

Isotopic exchange was performed by bombardment of the Be:H layer with D$_2^+$ ions (this ion fraction provides the highest flux) with energies of 5 keV per deuteron. Although such energy does not correspond to the common range of energies 50−500 eV of ions impinging the walls of a tokamak during the conditioning [5?], it was chosen to obtain a deeper implantation profile (~120 nm) which is better resolved by the surface analysis techniques. The samples were exposed to doses between 10^{20} and 10^{21} D/m^2 at surface temperatures of either 27 °C or 100 °C. During exposure a slit diaphragm covers partly the sample; the ion beam density is homogeneous within a 4 mm circle in the center of the sample, decaying linearly towards the edges of the sample.

In order to quantify the amount of hydrogen isotopes in Be coatings and to obtain the depth profiles, two Nuclear Reaction Analysis (NRA) methods are chosen. The first one uses ^{1}H(^{15}N,αγ)^{12}C reaction for the post-mortem H profiling of the studied samples in Ruhr-Universität Bochum, Germany [17]. It allows a depth resolution of ~4 nm close to the surface. The size of the beam spot is approximately 2–3 mm, hence the hydrogen profiles are measured at two positions: in the center of the sample (maximum irradiation dose) and at the masked edge (not exposed). For D depth profiling ^{4}He Elastic Recoil Detection Analysis (ERDA) and the D(^{3}He,α)p NRA reaction were applied at IPP Garching, Germany [18]. The beam spot is 1x1 mm and 1x3 mm, respectively. The depth resolution is ~50–100 nm for these methods in Be.

4. Model comparison with the experiment

The ion beam irradiation experiment was used to validate the DITMIX model. Figure 1 shows both experimental data and modelled curves for hydrogen isotope profiles for a sample exposed to 10^{21} D/m^2 at room temperature. The error bars of the experimental data originate from a statistical error in the NRA measurements of hydrogen concentration at each depth. Erosion rate 8·10^{-6} nm/s is negligible in this experiment as the ion flux is only 1.6·10^{17} D/m^2/s. The starting H profile (denoted by t = 0 in Figure 1) is almost flat with an average value of H/Be = 0.037. However, there are two

distinctive features at the interfaces:

- The large concentration of hydrogen is present within 10–15 nm at the surface that drops with depth. This can be explained by a BeO layer at the surface [19], which limits the surface release of hydrogen to some extent and thus accumulates it. In order to take into account this effect in the model, w_{max}^k is increased 1.5 times within the BeO layer. In addition, the hydrogen diffusivity D is modified in this layer in accordance with the data from [19] as $7 \cdot 10^{-6}$ m^2/s $\times \exp(-2.1$ eV$/kT)$. The hydrogen-containing impurities on the surface (H$_2$O, C$_x$H$_y$) may also contribute significantly to the measured peak of H concentration. This is not taken into account by the model and is one of the uncertainties of the experiment.

- At the rear interface there is a minor peak of H concentration at 500 nm and a substantial decrease in the deeper layers. This is due to the 100 nm surface roughness of a tungsten substrate: there is less beryllium within the range of 500 to 600 nm to accommodate hydrogen. Hence, in the model a depth profile of w_{max}^k was modified to allow less traps at the rear interface.
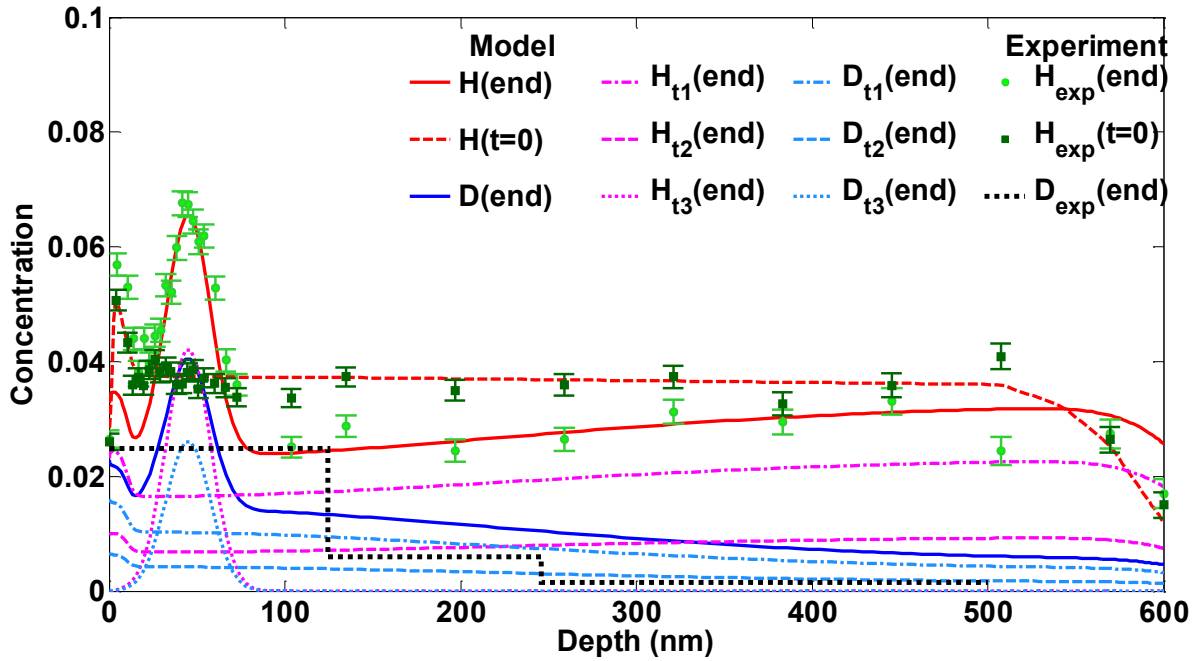

Figure 1. Hydrogen isotope depth profile for a Be:H co-deposit exposed to 10^{21} D/m^2 at 27 °C: modelled and measured by ^{15}N-NRA (H$_{exp}$) and ^{4}He-ERDA (D$_{exp}$). The indexes t1, t2, t3 refer to the trap type.

The peak of the H concentration in the exposed sample at 45 nm originates from the ion-induced defects, produced during the bombardment with high energy ions. Therefore, a third type of traps with the highest de-trapping barrier of 2.0 eV (as observed in similar ion beam experiments in [20]) was introduced in the model in addition to two intrinsic traps described in [10]. The concentration of the ion-induced traps w_{max}^3 is allowed to grow linearly with the D irradiation fluence in the model; these

7

traps are produced locally in the implantation zone with a normalized Gaussian distribution. Both protons and deuterons may enter these trapping sites and cannot be released if the surface temperature is lower than 700-800 K [20].

The most remarkable feature of the hydrogen depth profile in Figure 1 is a decrease of H concentration deep in the bulk. This presumably indicates H $\rightarrow$ D isotopic exchange behind the implantation zone ($x > 120$ nm). It is a fluence dependent process, as sample exposed to 10^{20} D/m^2 did not evidence such decrease at all. The kinetic de-trapping mechanism (equation 4) obviously cannot account for this as it applies only in the implantation zone; in fact, it was found to have a negligible influence on the modeling result with $\sigma_{kin} = 3 \cdot 10^{-16}$ cm^2. The swapping mechanism (equation 5) has only a minor smoothing effect on the H profile compared to the modelling case when the swapping is disabled. E_{swap}^k is set to 0.1 eV in the calculations. Hence, another mechanism, related to the hydrogen transport, governs the isotope exchange in the Be coating. In order to reproduce the experimental data, the maximum allowed concentrations of traps with $k = 1, 2$ w_{max}^k was limited in such a way that the initial Be:H co-deposit is almost saturated with hydrogen, while the ratio between the trap populations $w_{max}^1/w_{max}^2 = 0.4$ was kept the same as in [10]. Consequently, the total hydrogen content in the bulk Be layer in the model is limited to H/Be = 0.038. The coatings deposited in the magnetron are rather dense, with a measured density of $1.17 \cdot 10^{29}$ at/m^3, which is close to that of a pure beryllium $n_{Be} = 1.24 \cdot 10^{29}$ at/m^3. The co-deposits in tokamaks are usually less dense, in particular surface analysis of Be co-deposits at the cold (< 100 °C) apron of the tile 1 in JET showed density less than 10^{29} at/m^3 with D/Be $\approx$ 0.1 [21].

Despite a low resolution in depth, ^{4}He-ERDA measurements shown in Figure 1 show less agreement in the bulk with the modelled D profile, casting some doubt on the processes involved in the model.

The measured total H and D content in three different samples, is given as a function of the D fluence in Figure 2, together with the modelled curves. The D content measured by NRA agrees well with the model, showing a substantial rise of the implanted D in the coating with irradiation dose. In fact, 70–90% of the implanted deuterium stays retained in the sample. The data points on the H content agree reasonably well with the modelled curve (except for the measurement at $5 \cdot 10^{21}$ D/m^2), if the surface peak of H (see Figure 1) is disregarded. Therefore, this peak most likely originates from the impurities on the surface than from any process related to the isotopic exchange.

The impact of temperature on isotopic exchange is illustrated in Figure 3, where measured and calculated hydrogen profiles are given for a similar Be:H layer exposed to 10^{21} D/m^2 at 100 °C. The modelled curve is in a reasonable agreement with the experimental data. Heating the surface to 100 °C leads to a more intensive H removal via isotopic exchange compared to the case at room temperature. The model predicts that thermal release of hydrogen from the Be:H coating at 100 °C is not enough to

account for such removal. Hence the isotopic exchange does not only depend on fluence as shown in Figure 2 but it is also thermally activated.
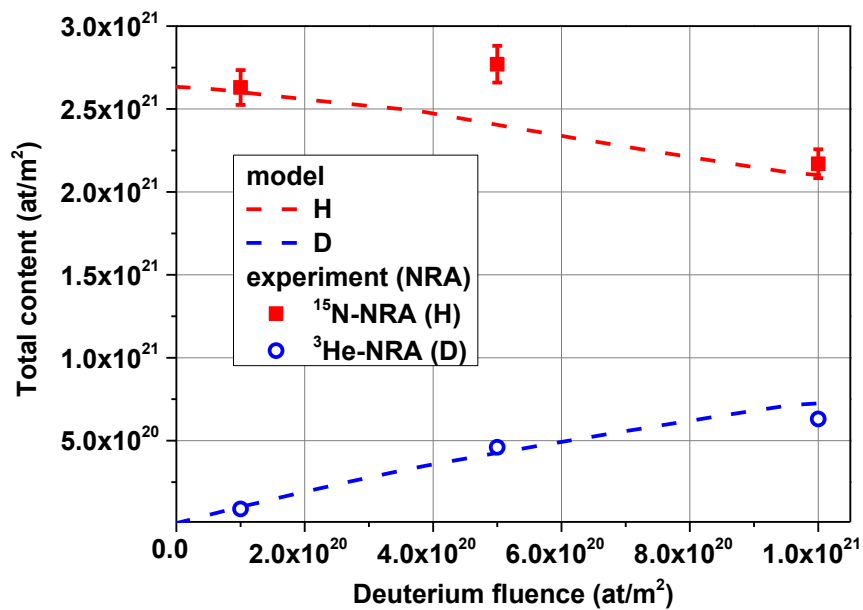

Figure 2. Total content of H and D atoms in the samples exposed at room temperature as a function of D fluence. Surface peak of hydrogen is disregarded.
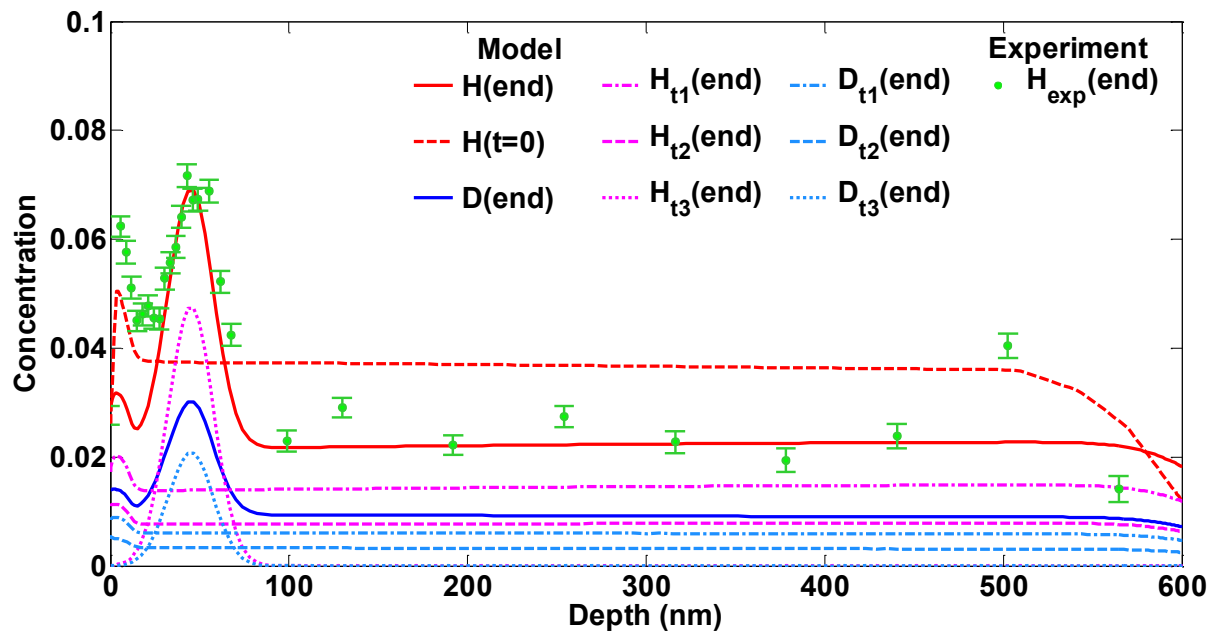

Figure 3. Hydrogen isotope depth profile for a Be:H co-deposit exposed to 10^{21} D/m^2 at 100 ºC: modelled (lines) and measured by ^{15}N-NRA (points). The indexes t1, t2, t3 refer to the trap type.

5. Discussion

The mechanism of the isotopic exchange predicted by the model in agreement with the experiment

can be summarized as follows. The implanted deuterium firstly accumulates in the implantation zone in the soluted state. As the trapping sites in the Be:H co-deposit are almost saturated, even a minor release of hydrogen due to the thermally activated de-trapping leads to its substitution in the trap by deuterons.

The model predicts that thermal release from the trap of type $k = 1$ ($E_r^1 = 0.790$ eV) is already high at room temperature. It can be easily seen if the right hand side of equation 3 is modified in a way that only thermal de-trapping is present: $\partial w_i^1/\partial t = -v_r^1 w_i^1 \exp(-E_r^1/kT)$. The solution of this equation is an exponential decay of H concentration w_i^1 in the trap of type $k = 1$ with a characteristic e-fold time $\tau = [v_r^1 \exp(-E_r^1/kT)]^{-1} \approx 5$ s. Therefore, if no trapping occurs, the trap of type $k = 1$ quickly becomes empty even at room temperature. In the presence of trapping term all released hydrogen is immediately re-trapped; the characteristic time of re-trapping is comparable to the de-trapping time. Therefore, in the thermal equilibrium at $T \geq 300$ K some part of the trapped H is constantly released and re-trapped, so that the resulting H profile is stable in time. If at the same depth there is a significant amount of soluted D, it can easily get trapped instead of H atoms, hence isotopic exchange occurs.

The released hydrogen diffuses either to the surface or to the bulk, followed by the diffusing deuterium. In case of a high energy (keV) irradiation a new type of the trap is produced within the implantation zone, which captures all passing H and D atoms due to its high de-trapping barrier; thus, the surface release of hydrogen is limited not only by recombination, but also by trapping in the ion-induced traps. The soluted hydrogen population which moves to the bulk of the coating reaches the rear interface and stops; as H solubility is limited, a uniform profile of soluted H is established all over the coating. Substantial increase of the number of implanted D atoms, which propagate all over the sample, leads to an increased probability of the H → D substitution in the traps. It should be reminded that [3]He-NRA and [4]He-ERDA did not confirm such deep propagation of the D atoms in the sample, casting some doubt on the isotopic exchange mechanism described here.

6. Conclusion

In order to understand the interaction mechanisms between hydrogenic species and beryllium co-deposits, a 1D DIffusion/Trapping Model of Isotopic eXchange in Be (DITMIX) is developed and the modelled hydrogen isotope depth profiles are compared with the experimental ones.

DITMIX predicts that the governing factors for the isotopic exchange are fluence and temperature; the latter affects hydrogen transport rates through Arrhenius terms. As far as tritium removal in Be co-deposits in ITER is concerned, the model suggests to use H_2 or D_2 wall conditioning discharges with high ion fluxes and/or longer exposure times combined with baking of the vacuum chamber. It should be mentioned that a proper evacuation of the isotopes released from the chamber wall is necessary to

avoid fuel re-implantation, which is neglected in the present model.

Acknowledgments

References

[1] R. Doerner et al., Nucl. Fusion **49**, 035002 (2009).

[2] S. Brezinsek et al., Nucl. Fusion **53**, 083023 (2013).

[3] A. Widdowson et al., Phys. Scr. **T159**, 014010 (2014).

[4] A. Baron-Wiechec et al., J. Nucl. Mater. (2015), doi:10.1016/j.jnucmat.2015.01.038.

[5] D. Douai et al., J. Nucl. Mater. (2014), doi:10.1016/j.jnucmat.2014.12.034

[6] T. Wauters et al., J. Nucl. Mater. (2014), doi:10.1016/j.jnucmat.2014.12.097

[7] O. V. Ogorodnikova et al., J. Nucl. Mater. **273**, 66 (1999).

[8] G. Longhurst: *TMAP7 User Manual.* Idaho, US, 2008.

[9] K. Schmid, V. Rieger, and A. Manhard, J. Nucl. Mater. 426, 247 (2012).

[10] M. Baldwin, T. Schwarz-Selinger, and R. Doerner, Nucl. Fusion **54**, 073005 (2014).

[11] R. A. Causey, J. Nucl. Mater. **300**, 91 (2002).

[12] M. Pick and K. Sonnenberg, J. Nucl. Mater. **131**, 208 (1985).

[13] N. N. Trifonov, D. K. Kogut, and V. A. Kurnaev, J. Surf. Investig. X-ray, Synchrotron Neutron Tech. **2**, 175 (2008).

[14] A. Allouche et al., J. Phys. Chem. C **114**, 3588 (2010).

[15] K. Schmid, U. von Toussaint and T. Schwarz-Selinger, J. Appl. Phys. **116**, 134901 (2014).

[16] N. V. Mamedov: *Method of research of plasma-surface interactions based on the ion scattering spectroscopy and installation for its implementation*. Ph.D. thesis, MEPhI, Moscow, 2013.

[17] F. Traeger et al., Phys. Rev. B **84**, 075462 (2011).

[18] M. Mayer et al., Nucl. Instrum. Methods B **267**, 506 (2009).

[19] M. C. Billone et al., Fusion Eng. Des. **27**, 179 (1995).

[20] M. Reinelt et al., New J. Phys. **11**, 043023 (2009).

[21] S. Brezinsek et al., J. Nucl. Mater. (2015), doi:10.1016/j.jnucmat.2014.12.007